RADIO SCIENCE INVESTIGATIONS WITH VOYAGER

V. R. ESHLEMAN and G. L. TYLER
Radioscience Laboratory, Stanford University, Stanford, CA 94305, U.S.A.

J. D. ANDERSON, G. FJELDBO, G. S. LEVY and G. E. WOOD
Jet Propulsion Laboratory, California Institute of Technology, Pasadena, CA 91103, U.S.A.

and

T. A. CROFT
Radio Physics Laboratory, Stanford Research Institute, Menlo Park, CA 94025, U.S.A.

(Received 24 May 1977)

Abstract. The planned radio science investigations during the Voyager missions to the outer planets involve: (1) the use of the radio links to and from the spacecraft for occultation measurements of planetary and satellite atmospheres and ionospheres, the rings of Saturn, the solar corona, and the general-relativistic time delay for radiowave propagation through the Sun's gravity field; (2) radio link measurements of true or apparent spacecraft motion caused by the gravity fields of the planets, the masses of their larger satellites, and characteristics of the interplanetary medium; and (3) related measurements which could provide results in other areas, including the possible detection of long-wavelength gravitational radiation propagating through the Solar System. The measurements will be used to study: atmospheric and ionospheric structure, constituents, and dynamics; the sizes, radial distribution, total mass, and other characteristics of the particles in the rings of Saturn; interior models for the major planets and the mean density and bulk composition of a number of their satellites; the plasma density and dynamics of the solar corona and interplanetary medium; and certain fundamental questions involving gravitation and relativity. The instrumentation for these experiments is the same ground-based and spacecraft radio systems as will be used for tracking and communicating with the Voyager spacecraft, although several important features of these systems have been provided primarily for the radio science investigations.

1. Introduction

The radio science investigations which are discussed here are based on the use of the spacecraft and Earth-station radio systems which are also used for two-way radio communications with, and tracking of, the spacecraft. The authors are the members of the NASA-selected experiment team charged with the responsibility for planning and conducting these investigations. (While the title 'radio science' is used for this team and investigation area, it should be noted that the planetary radio astronomy and plasma waves investigations discussed elsewhere in this issue, use experiment packages which also make radio wave measurements.) An important task of the experiment team is to help optimize the communications and tracking systems, the planned spacecraft trajectories, and the mission operations for the radio science investigations. However, this must be done in competition with the many other mission and science requirements so that ideal conditions for the science measure-

Space Science Reviews **21** (1977) 207–232.

ments will be achieved only rarely. Nevertheless, the Voyager missions incorporate major improvements in radiometric capabilities and provide major new target and experiment opportunities for radio science.

In the remainder of this section we outline the principal factors that control what can be achieved with the Voyager radio science investigations, and also introduce the experiments. The following sections treat in order: atmospheres and ionospheres; the rings of Saturn; gravitational fields; the solar corona and interplanetary medium; experimental relativity; and the radio science instrumentation.

Salient features of the Voyager radio science investigations are: the use of harmonic, dual-frequency, high-power, spacecraft transmissions at 13 cm-λ (S-band) and 3.5 cm-λ (X-band); the use of new, highly-stable, temperature-controlled, radiation-hardened quartz, spacecraft frequency standards; improved phase, group-delay, and amplitude stabilities in the spacecraft and ground radio systems; a novel attitude-control thruster configuration that minimizes accelerations along the Earth-spacecraft line-of-sight; and planned trajectories that provide multiple planetary and satellite encounters with radio occultations by Jupiter, Saturn and its rings, Titan, Uranus, and possibly Callisto.

In general, the radio observables are the frequency, group delay, intensity, and polarization of the radio signals which have been propagated over the spacecraft-Earth path. Measurements of these signal characteristics, their interrelationships, and their comparative values at the two carrier frequencies, can provide a rich mine of information about the regions traversed by the radio paths, and about forces that buffet the spacecraft and alter its motion. The results of these measurements will be used in investigations that represent both established types of experiments, which however will be conducted at new levels of precision on new planetary targets, as well as more speculative new areas of exploration.

Radiometric stability and precision are of utmost importance for the experiments. For example, measurement of changes in the received radio frequency to an accuracy of one part in 10^x of the transmitted frequency, for representative flyby conditions, can correspond to the detection of a change on the order of 10^{4-x} radians in the angle of refraction of the radio rays in occultation experiments. Such angular changes can be related directly to the detailed structure of the planetary atmosphere or ionosphere, as discussed below. Similar sensitivity to changes in both the angle and relative magnitude of the spacecraft velocity vector will provide accurate measurements of the causative gravity fields. For Voyager, the value of x will vary between about 11 and 14 depending upon operating mode and period of measurement.

When a spacecraft moves behind a planet as viewed from Earth, the radio paths traverse the planet's atmosphere and ionosphere, and for Saturn, can also probe its system of rings. All of these regions will affect the characteristics of the received radio signals, making possible the study of the vertical structure of these atmospheric regions, clouds, small and large scale variations associated with turbulence and weather, and fundamental characteristics of the ring particles and their disposition

around Saturn. The atmosphere and ionsphere of Titan will also be studied by such occultation measurements, and it may be possible to conduct a measurement of the ionosphere of Callisto. It is also expected that a reflection from the surface of Titan near the limb will be obtained during the occultation measurements. The radio ray paths always traverse the interplanetary medium, and each year they will pass near the Sun, making possible the study of the solar wind in both the inner and outer Solar System, the density and dynamics of the solar corona, and the relativistic signal delay caused by the Sun's gravity field. The gravity fields of the planets and satellites encountered by the spacecraft will affect their paths and hence the frequency of the radio signals, making possible the study of the fields for new information on the average mass density of the satellites and the internal structure of Saturn and Uranus. The spacecraft oscillators will appear to change frequency when the spacecraft are in the gravity fields of the major planets, making possible a gravitational red shift experiment. There are several other experiments involving relativity which are probably beyond the capability of the Voyager instrumentation, but which nevertheless are being considered because of their intrinsic importance and because of uncertainties in either the theoretical predictions or the ultimate system capabilities. These include the possibility of detecting, or setting important limits on, differences in the gravitational and inertial masses of the major planets, the rotation of inertial coordinates near a massive spinning body, and gravitational radiation.

2. Atmospheres and Ionospheres

Flyby trajectory characteristics of the two Voyager spacecraft at Jupiter and Saturn provide a good combination of conditions for radio occultation studies of their atmospheres and ionospheres. Figure 1 illustrates the paths of the radio image of the spacecraft as seen from Earth for the nominal JST and JSX trajectories. Note that both equatorial and polar regions will be probed, and that there will be both near-central occultations and more grazing occultations in which the spacecraft sets or rises, as seen from the Earth, at large angles from the local vertical at the occulting body. Figure 2 provides a side view of the occultation geometry in a rotating plane that instantaneously contains the earth, the spacecraft, and the center of the planet. The Saturn figure is illustrated to scale, while for Jupiter there is a 10 : 1 compression factor in the direction to Earth. Occultation distances from the planetary limb to the spacecraft range from about 6 to $20R_J$ (Jupiter radii) at Jupiter, and from about 3 to $6R_S$ (Saturn radii) at Saturn. In addition to these illustrated occultations, two near-equatorial regions of Titan's atmosphere and ionosphere will be measured, and there will be a radio occultation experiment at Callisto if there should be a delay of 10 days or more in the first launch. Experiments based on occultation of Voyager 2 by Uranus are also being planned. An inherent characteristic of all of these outer planet occultations is that the solar zenith angle at the measured regions will be near 90 degrees.

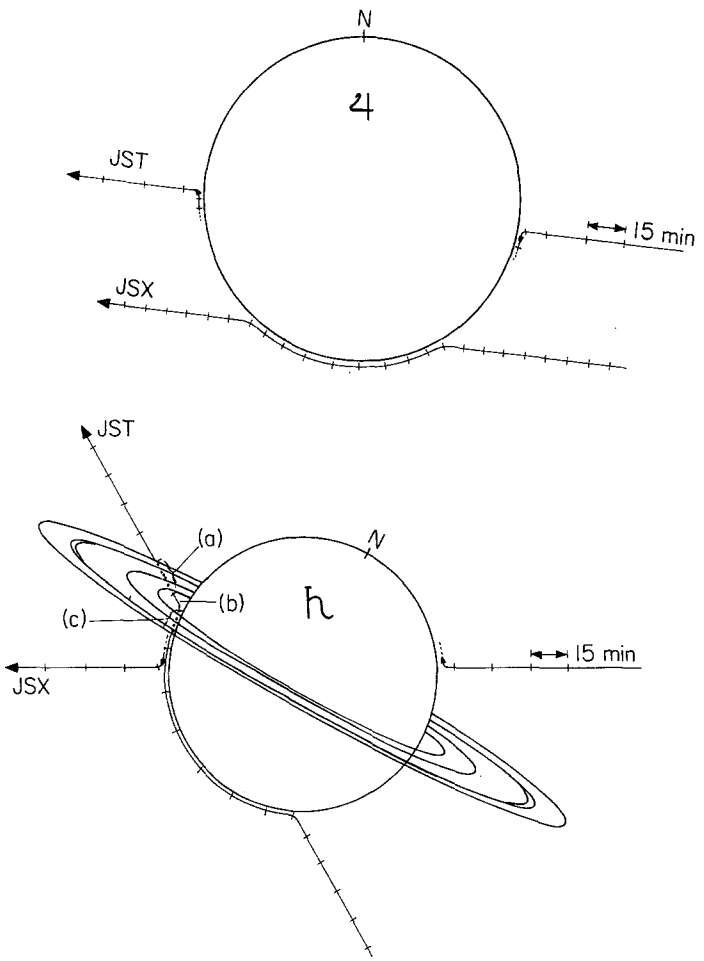

Fig. 1. View from Earth of Voyager occultations at Jupiter and Saturn. The spacecraft radio images follow the indicated paths for the JST and JSX trajectories at Jupiter and Saturn. Note that there is a combination of near central and more grazing occultations at both planets. For JST at Saturn, region (a) provides a clear occultation of the rings and (b) a clear atmospheric occultation, while (c) is a combined ring and atmospheric occultation.

2.1. Vertical atmospheric structure

For a central passage of a spacecraft behind a planet, the trajectory would dip to zero in the vertical scale of Figure 2. At occultation entry and exit, the spacecraft would appear from the Earth to set and rise approximately normal to the limb of the planet, and the atmosphere would be sampled with height along a near-vertical path. Such a central passage is the optimum condition for occultation measurements of the vertical structure of the atmosphere. The JST trajectory at Jupiter and the JSX (Uranus) trajectory at Saturn are near optimum in this regard. The other two trajectories give occultation conditions in which the virtual image of the spacecraft

enters the atmosphere along a path well away from the vertical. After modest penetration into the atmosphere, the spacecraft image as viewed from Earth will move approximately horizontally through the atmosphere, over south polar regions in both cases, with spacecraft rise at emersion being over a different part of the planet. While such non-central occultations will produce reliable vertical profiles over a smaller range of heights than is the case for central occultations, they can be very useful in sampling conditions over a wide range of latitudes, in studying complex atmospheric structure due to turbulence and weather, and in helping to determine possible distortion of gravitational equipotentials from oblate spheroids, as discussed below. Also, the more distant JSX occultation at Jupiter may be useful in measuring the tenuous high regions of the atmosphere to greater precision than is possible with closer occultations.

Figure 2 also shows illustrative radio ray paths in the regions behind the planets. Measurements of the received frequency of the radio signals from the spacecraft can provide precise information on the angle of refraction in the planetary atmosphere.

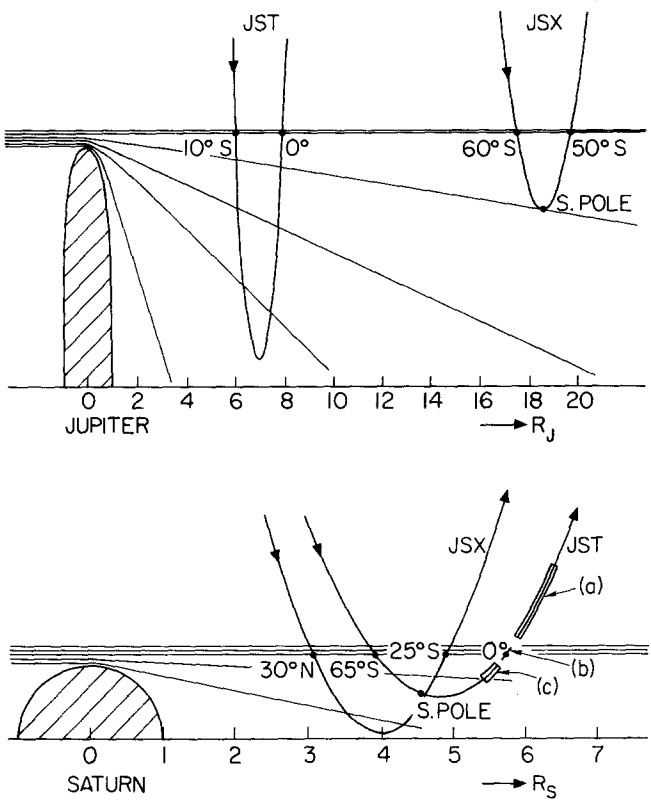

Fig. 2. Side view of Voyager occultations at Jupiter and Saturn. The trajectories are plotted in a rotating plane that instantaneously contains the Earth, the spacecraft, and the center of the planet. There is a reduction factor of 10 in the direction to Earth for the Jupiter illustration, while the two figure dimensions have the same scale for Saturn. The latitudes of occultation immersions and emersions are shown, and regions (a), (b), and (c) of Fig. 1 are also illustrated here.

Knowledge of this angle as a function of time, together with the spacecraft trajectory, makes it possible to estimate the refractivity of the atmosphere as a function of height. (Refractivity $\nu = n - 1$, where n is the refractive index.) The profile of refractivity in turn can be used to determine the relative temperature and pressure as a function of height, and such relative profiles can be made absolute from knowledge of the atmospheric constituents (Fjeldbo and Eshleman, 1965; Kliore *et al.*, 1965; Eshleman, 1965).

The process of converting the measured signal frequencies into a height profile of refractivity, or a more general two- or three-dimensional refractivity model of the atmosphere, is not straightforward and in general cannot yield a unique result. The problem of determining refraction angles from any given atmospheric model is, by comparison, both straightforward and unique. Unfortunately, our problem is the hard one. If one imposes the assumption that the atmosphere is spherically symmetric, there is a mathematical transform pair that allows computations in either direction, and in this case the profile computed from the refraction angles is the correct and only answer (Fjeldbo *et al.*, 1971). We are not aware of any other potentially applicable model where such a direct mathematical inversion has been identified. A different approach involves iteration downward in an atmosphere modeled by successive thin layers within each of which the refractivity is constant. While such a method has been used for the spherical case (Fjeldbo and Eshleman, 1968), it is potentially applicable with further development to any geometrical complexity that can be modeled in this way. The radio science team is preparing for both types of inversion approaches for the Voyager occultation experiments. The departure from spherical symmetry due to the oblateness of the major planets will be treated both by using a sequence of offset spherically-symmetric models to match the curvature of the equirefractivity profiles at the occultation points (Kliore and Woiceshyn, 1976), and by the iterative process applied to the oblate spheroidal geometry. It is expected that this latter method may be made more complete with attempts to treat possible zone-belt differences and particular spot features in the atmospheres.

Important additional information about atmospheric structure can be obtained from the intensity of the dual-frequency signals received during occultation. Figure 2 illustrates the effects of differential refraction on intensity by showing that evenly spaced parallel rays to Earth connect with increasingly spread rays at the spacecraft for progressively lower ray passages through the atmosphere. Thus signal intensity decreases as the rays penetrate deeper into the atmosphere. Measured signal intensity can be inverted as discussed above for the frequency measurements, and should yield the same refractivity profiles if the changes in intensity are due solely to such atmospheric defocussing (Fjeldbo *et al.*, 1971). However, there are two other factors to consider, as discussed below.

Certain errors in profiles derived from Doppler frequency measurements undergo an inherent magnification deep in the atmosphere, but this does not occur in the intensity inversion process (Hubbard *et al.*, 1975; Eshleman, 1975). Thus cross-checks can be made to determine the onset of such magnified errors, with the possible

result that the characteristics of such an error source could be measured. For example, profiles determined from Doppler measurements during the non-central occultations will be very sensitive to the assumed orientation of the local vertical (Hubbard *et al.*, 1975). At atmospheric levels where the signal intensity is reduced by a factor M (which could reach values of thousands), an error in the local vertical of δ radians would produce a temperature error on the order of $200M\delta$ percent when the spacecraft sets or rises at an angle of 45° from the vertical (Eshleman, 1975). But if the temperature were known more accurately than this from the intensity measurements, or from other Voyager experiments, then the apparent error could provide information on the orientation of local equipotentials to an accuracy which could be important in the study of gravitational anomalies due to internal structure and atmospheric currents. The accuracy of the local vertical of the global field of Jupiter as determined with Pioneer spacecraft is about one minute of arc (Anderson, 1976).

The second factor relative to the use of signal intensity measurements is that atmospheric absorption would add to defocussing loss, but these two effects would be separable whenever the refractivity profile can be determined from the Doppler measurements (Fjeldbo *et al.*, 1971). Microwave absorption in the atmospheres is expected due to cloud condensates, their vapors, or principal atmospheric constituents at low altitudes and hence high densities. The loss profile measured at the two radio frequencies would provide information on the location, density, and other characteristics of the clouds or other absorbing material.

Before absolute pressure and temperature profiles can be derived from the refractivity data, one must know either the composition or the temperature at some altitude level. For the Voyager missions, the IR and UV sensors are expected to yield complementary data on these parameters. Additional information may be obtained from the signal intensity measurements. For instance, if the altitude level of ammonia clouds could be identified in a microwave loss profile, one would know the approximate temperature at this altitude based on considerations involving vapor saturation. This temperature information would, in turn, allow us to use the scale height of the refractivity profile near the cloud level to estimate the mean molecular mass of the atmosphere. The mean molecular mass could in turn be utilized together with other data to establish limits on the abundance ratios between the principal atmospheric constituents.

The atmospheric occultation experiment is of special interest for Titan, the only satellite known to have an appreciable atmosphere. The planned trajectory for the JST mission includes a near central passage behind Titan, under conditions which are favorable for vertical profile measurements. While there is considerable uncertainty about atmospheric conditions at Titan (Hunten, 1974), it is expected that the radio occultation experiment can provide important atmospheric results over a wide range of altitudes, probably including conditions from the surface to heights where the atmospheric pressure is on the order of 1 mb. At greater heights, ionospheric measurements would provide additional information as discussed below.

The occultation geometry at Uranus has not yet been specified. A central occultation at relatively short limb-spacecraft range is desirable in order to probe as

deep as possible into the atmosphere and determine both refractivity and absorptivity profiles. It appears lilely that atmospheric measurements at Jupiter, Saturn, and Uranus will provide profiles from pressure levels on the order of 0.1 mb to the level where absorption becomes the limiting factor, possibly in the 1 to 10 bar region. That is, even at the distance of Uranus, radio signal intensity is not expected to be a limiting factor in the range of altitudes that can be studied using relatively short occultations distances.

2.2. Ionospheric profiles

The ionospheres of Jupiter, Saturn, and Titan are to be measured by the radio occultation technique, with the added possibility that such observations will also be made at Uranus and Callisto. Accurate ionospheric electron concentration profiles can provide important clues about the photochemistry, temperature, constituents, dynamics, and structure of planetary upper atmospheres, and about other sources of ionizing energy such as precipitating magnetospheric particles and the infall of meteoric particles.

The vertical profile of free electron concentration in an ionosphere can be found from the profile of refractivity, which in turn is determined in the same general way as described previously for the refractivity of the neutral atmosphere. However, there is an important difference in that the refractivity is also proportional to the square of the radio wavelength for ionospheres, while it is essentially independent of wavelength for neutral atmospheres. Thus the dual frequency measurements will be self-calibrating in the sense that ionospheric profiles derived from Doppler frequency differences will be independent of trajectory uncertainties and spacecraft oscillator instabilities (Fjeldbo *et al.*, 1965).

Another source of error in occultation experiments arises due to an incorrect assessment of changes in the interplanetary medium and terrestrial atmosphere and ionosphere along the radio path. This problem can be minimized by tracking the spacecraft which is not being occulted, because the terrestrial and interplanetary media should be similar along the two paths. Other independent measurements of the Earth's atmosphere and ionosphere will also be used for this purpose. For example, the terrestrial ionospheric electron content can be monitored through observation of geostationary satellite signals.

The illustrations of Figure 2 also apply for ionospheric occultation except that the bending is very slight; no attempt was made in this figure to represent such ray paths. While slight, ionospheric bending is both up (in the topside of each ionospheric layer) and down (in the bottomside of each layer), with the result that ray crossings (caustics) occur and several propagating modes will often be present simultaneously. In the Pioneer 10-11 occultation experiments this multi-mode condition was prevalent due to the multi-layered structure of the Jovian ionosphere, and made a useful characterization of the lower parts of the ionosphere difficult to obtain (Fjeldbo *et al.*, 1976). Multiple modes will tend to be more numerous in the Voyager 13 cm-λ measurements because the spacecraft will be further from the planet, but at 3.5 cm-λ

they will tend to be less prevalent because of the λ^2 dependence of the refractivity of the plasma. It is of particular significance that the signal to noise ratios for Voyager will exceed the Pioneer 13 cm-λ value by about 10 and 23 dB at 13 and 3.5 cm-λ, respectively. Methods for sorting out multiple modes depend critically on signal intensities, and the dual-wavelength signatures can be of further help in this regard (Croft, 1976). Proper interpretation of the ionospheric measurements is important not only for deriving valid profiles for the lowest regions in the ionosphere, but also for determining accurate starting conditions for the derivation of the high altitude part of the profiles for the neutral atmosphere.

2.3. Atmospheric structure associated with turbulence and weather

In the derivation of atmospheric and ionospheric profiles from measurements of signal frequency or intensity, changes of refractivity with height can be determined only if the variations in other directions are specified. In the absence of other information, one would assume a steady-state, stable distribution with equirefractivity surfaces normal to gravity. With this assumption, there is a one-to-one correspondence between all of the variations in the measured frequency or intensity, and horizontally-stratified features in the derived temperature and pressure profile. But the question arises whether all of the signal variations are in fact due to such static, horizontally-stratified, atmospheric features; some may be due to more complex spatial and temporal variations of refractivity, such as would be associated with planetary weather and atmospheric or ionospheric turbulence. If such three-dimensional structure is present, it would cause both fluctuations in the derived temperature and pressure from the true values, and also average errors or biases.

Increasing attention is being given to these problems for both radio and optical occultation investigations of planetary atmospheres. While much more remains to be done, we believe several important conclusions about this subject can be made at this time.

It appears that some of the detailed and strong excursions seen in the occultation measurements at Venus, for example, are due to global, horizontally-stratified, atmospheric structure, corresponding to abrupt changes in the temperature lapse rate and perhaps to boundaries of tenuous cloud strata. The same features are seen at different parts of the planet and in measurements taken years apart (Fjeldbo *et al.*, 1971; Howard *et al.*, 1974).

While concern has been expressed that turbulence could cause large errors in derived atmospheric profiles (Hubbard and Jokipii, 1975; Young, 1976), there are claims that the analytic bases for this concern are incomplete and that the resulting conclusions are overly pessimistic (Eshleman and Haugstad, 1977; Haugstad, 1977). The latter authors conclude that errors in normalized temperature and pressure due to atmospheric turbulence, under conditions where there is no multipath propagation, vary from much less than, to comparable with, the fractional root-mena-square fluctuations in refractivity. Hence the errors are expected to be small for nominal assumptions concerning the turbulence (Haugstad, 1977). Also, *in-situ* results at

Mars and Venus indicate that derived occultation profiles are compatible with the direct measurements to the accuracy of the different experiments.

For the frequency and intensity fluctuations that are caused by turbulence, power spectra obtained from dual-frequency measurements are expected to have characteristic shapes that would verify that the fluctuations were indeed due to turbulence. Such spectra would also make it possible to specify important parameters (intensity, scales, variations with height) of the atmospheric or ionospheric turbulence (Woo and Ishimaru, 1974; Haugstad, 1977).

While the near-vertical occultations of JST at Jupiter and of JSX at Saturn are preferred for vertical profile measurements, the other more nearly grazing occultations may provide better information on non-horizontally stratified atmospheric structure over a wide range of latitudes. The central parts of such occultations involve nearly horizontal motion of the lowest part of the radio ray paths through the atmosphere. Signal intensity and frequency variations under this condition cannot be caused by horizontally stratified features. Spectral characteristics that do not fit possible turbulence models would be due to other large-scale atmospheric structure which, by analogy with the terrestrial atmosphere, might be said to be a manifestation of weather on the planet.

3. Rings of Saturn

The Voyager encounters with Saturn provide an opportunity to study the ring system with radio occultation techniques. The JST trajectory includes a Saturn ring occultation following atmospheric occultation emersion. The JSX trajectory provides an optional retargeting for Titan encounter and ring occultation should the JST spacecraft fail prior to Saturn encounter.

The goals of these observations are to measure the complex (amplitude and phase) radio extinction and angular scattering function of the rings as a function of wavelength, polarization, and radial distance from Saturn. These observations would then be used to infer the first several moments of the ring particle size distribution, the total amount of material in the rings, the radial distribution of that material, and limits to possible particle shapes and constituents (Marouf, 1975).

As in atmospheric occultations, the 13 and 3.5 cm-λ radio waves will be transmitted from the spacecraft through the rings and received at Earth. The motion of the spacecraft will carry the geometric line of sight from the planetary occultation point within the eastern ansa (region (b) in Figures 1 and 2) outward through the entire ring system (region (a) in the figures). The complete phase, intensity, and polarization of the received signals at both wavelengths will be recorded at Earth. Note also from the figures that the complete ring plane will be crossed along a second path by the rays refracted through the atmosphere just prior to the atmospheric emersion of the spacecraft image (region (c) in the figures). This combined atmospheric and ring occultation will also be recorded.

It is expected that the received signal will consist of two principal components; a coherent signal that represents propagation directly through the rings, and an incoherent component which reaches the Earth by scattering from particles that do not lie along the geometric straight-line path to Earth (Eshleman, 1973). Even though the rings consist of discrete particles, they interact with the radio wave in such a way as to produce average effects (per unit volume) on wave intensity and phase, much as does an atmosphere or ionosphere of discrete molecules or electrons. For the coherent signal, the rings can be characterized by their effective wave propagation constants. The coherent and incoherent components will be recognized and separated in the data on the basis of their spectral, time correlation, and polarization characteristics.

The first-order effects expected are shown in Figure 3. At each wavelength, the coherent component will be shifted in phase and attenuated due to the effective propagation constants of the ring material. If the concentration of ring particles varies with radial distance from Saturn, the progressive change in phase would correspond to small changes in the angle of refraction, so that it appears as a

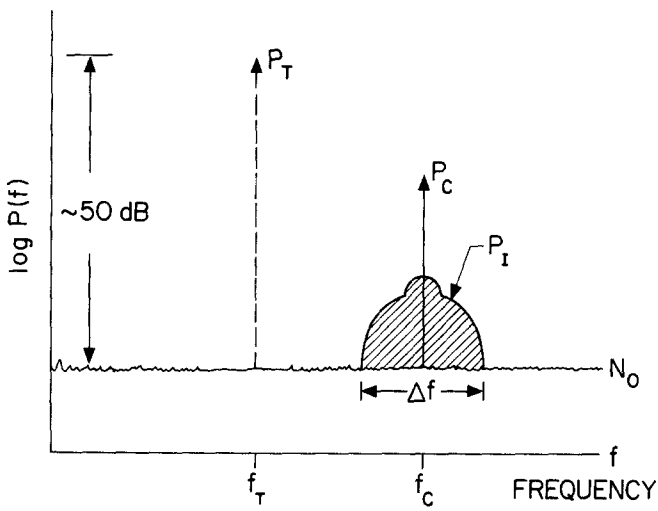

Fig. 3. Signal characteristics during Saturn ring occultation. Transmitted signal (P_T, f_T) is converted into coherent part (P_c, f_c) and incoherent part (P_I, Δf). System noise level N_0 is about 50 db below the received power in the absence of rings. Shape of incoherent spectrum schematically represents expected signature of a bimodal particle size distribution. Most scattering effects are wavelength dependent so that additional information is available by comparison of 13 and 3.5 cm-λ results. Variation of incoherent spectrum with polarization is not illustrated.

frequency shift in a manner that is analogous to an atmospheric occultation. Unlike atmospheric occultation, however, the reduction in the coherent signal intensity in ring occultation is expected to be due primarily to scattering of energy out of the direct path.

The phase of the coherent wave depends primarily on the total number of small particles per unit area projected normal to the spacecraft-to-Earth line-of-sight (i.e., the areal density). The precision of the phase data is limited by the oscillators employed. For frequency stabilities associated with the onboard oscillator, the threshold of detection would correspond to small ice particles whose areal density varies by about $20\,\mathrm{g\,cm^{-2}}$ in a period of about 1000 sec. Assuming a spacecraft velocity of $10\,\mathrm{km\,sec^{-1}}$ in the plane of the sky, this gives a sensitivity to gradients in material of $2\times10^{-3}\,\mathrm{g\,cm^{-2}\,km^{-1}}$, if the particles are small as compared with the radio wavelength.

The intensity of the coherent wave also carries important information about the ring particles. It appears that measurements of coherent signal extinction will be limited to an accuracy of about 10% at 3.5 cm-λ, and perhaps 1% at 13 cm, by systematic and slowly varying errors in spacecraft antenna pointing. For a simple model involving only optically thin regions and particles that are large relative to the wavelength, these errors would correspond to the same fractional error in the total projected area of the particles viewed against the plane of the sky. We estimate from current models for the B ring that this attenuation will be between 40 and 60 dB. As a result, the coherent wave may be below the limit of detection during portions of the ring occultation.

The incoherent signal illustrated in Figure 3 arises from scattering by ring particles with circumference greater than a wavelength. It can be analyzed in terms of the average angular scattering properties of the rings mapped into the frequency domain by the Doppler effect. This mapping can be understood in terms of the relative velocities between the spacecraft, ring particles, and the receiving station on Earth. Signals transmitted from the spacecraft illuminate ring particles at a frequency shifted by the instantaneous relative spacecraft-particle velocities. The component of the scattered wave that is re-radiated in the direction of the Earth undergoes a second shift in frequency determined by the velocity of the particle relative to that of the Earth. The JST trajectory at Saturn was chosen in part so as to align the loci of constant Doppler shifts with the circumferential ring coordinate over a limited region of the ring plane. An example of one such set of Doppler loci is shown in Figure 4. As illustrated, each slice of the incoherent spectrum is closely associated with a portion of the rings at a constant radius from Saturn's center of mass. We estimate that the radial resolution achieved at 3.5 cm wavelength will be about 100 km, approximately two percent of the radial dimension of the Cassini division between the A and B rings. At 13 cm-λ the resolution will be somewhat poorer due to the larger ring area illuminated at the longer wavelength, and the deviation of the Doppler loci from the ideal conditon over the larger area.

A critical factor in the ring occultation experiment is the size of the particles relative to the size of the spacecraft antenna (3.66 m diameter). If the predominant particle size is greater than the spacecraft antenna size, then the forward scattering lobe will be narrower than the spacecraft antenna beamwidth. In this case, most of the scattered energy can be observed with a simple geometry in which the spacecraft

antenna is always directed toward the geometric position of the Earth. However, particles smaller than the spacecraft antenna will produce forward diffraction lobes that are wider than the antenna beamwidth and no fixed condition of illumination

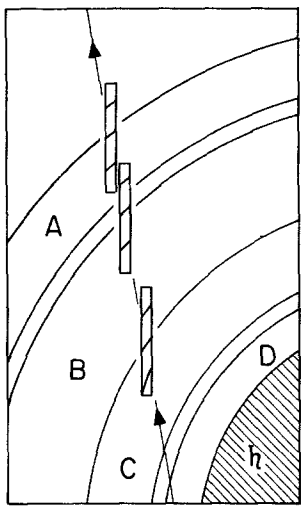

Fig. 4. Radial resolution for incoherent signals in Saturn ring occultation measurements. Figure represents ring plane with Saturn at lower right. Spacecraft is located below the plane of the rings out of the figure at the top of the page, Earth above the ring plane out of the figure at the bottom of the page. Directed line from lower right to upper left is the path of the geometric ray between spacecraft and the Earth. Boxes outline the ring plane area illuminated at three instants by the 3.5 cm-λ antenna pattern. The one-half power contour is approximately an ellipse with axes given by the rectangle. Curved lines approximately tangent to the circumferential coordinates of the rings are loci of constant Doppler shift separated by 1 kHz. Measurement resolution is on the order of 20 Hz. Similar figure obtains at 13 cm wavelength except antenna beam intersection is larger and contours deviate from circumferential condition.

will permit measurements of the entire scattering lobe. Current Earth-based radar observations indicate that many particles larger than about 2 cm in diameter are present in the rings, but give little hard information to constrain the upper size limits (Pollack *et al.*, 1973). We cannot now predict which of the alternatives above best represents the conditions we will encounter or even if such conditions will be the same for all parts of the ring system.

The radio science team is planning to conduct the JST ring occultation experiment with the antenna directed toward the Earth. This strategy will yield the maximum signal-to-noise ratio for the coherent component. It will also yield the mean particle size and information on the particle size distribution, particularly if most of the particles are a few meters in diameter or larger. The effects of particles in the centimeter-to-meter size range will be recognizable in the data, although detailed information will not be available on the distribution of sizes in that range. We plan to obtain information on the intermediate-scale particles by incorporating an oblique

scatter experiment in the JSX flyby, during which the spacecraft antenna will be directed toward the rings through a range of oblique scattering angles.

Polarization of the scattered waves is an independent observable which is germane to the study of the incoherent signal, and in principal, to the coherent wave as well. The polarization of the coherent wave will be modified by factors that depend primarily on particle shape if multiple scatter can be neglected, and by a combination of particle shape and multiple scattering in regions where the latter is important. Strong depolarization is observed in backscatter radar observations, and is one of the puzzling aspects of the ring system in these Earth-based experiments (Goldstein *et al.*, 1977). For the coherent wave, we know of no particular reason to expect strong polarization effects, but this could occur if non-spherical particles have ordered orientations.

Polarization measurements will be made with coherent receiving systems for right and left circular polarization at each wavelength. The data can be processed to determine the complete properties of the waves – intensity, axial ratio, and orientation of the polarized part, and the intensity of the unpolarized part – as a function of time and frequency. For the coherent signal, data processing based on polarization will improve the *a posteriori* signal-to-noise ratio.

The discussion above is expressed in terms of a simplified, single-scattering model. However, the fundamental experimental considerations of geometry and strategy do not depend on that model, but only on the assumption that the particles follow individual Keplerian orbits with few collisions. We expect to encounter a wide range of conditions as the radio beam moves outward through the ring system, and there may be no single scattering model or analysis technique which is appropriate over the full range. We are engaged in a continuing study of this experiment with emphasis on the sensitivity of data inversion to the experimental parameters, and on more complex models which include multiple scatter and polarization.

4. Gravitational Fields

Radio tracking observations of changes in the velocity vectors of the Voyager spacecraft, as they fly near the outer planets and their satellites, will be used to define the gravitational fields. These observations will be augmented with trajectory information derived from use of the Voyager optical systems. For each of the planets, the total mass and several higher mass moments can be determined, while only the total mass of a satellite is discernible. The results will be used to study interior models for the giant planets, the bulk density of the satellites, and the masses of the rings of Saturn.

The Pioneer 10 and 11 spacecraft came much closer to Jupiter than will the Voyager spaceraft, so that it will not be possible to improve upon the Pioneer gravitational results for Jupiter despite the improvements in the Voyager radio systems. However, Voyager should provide improved results on the masses of the

Galilean satellites. For example, Pioneer 10/11 tracking data were used to determine the masses of Io and Ganymede to an accuracy of about 0.5%, while Voyager should provide an accuracy of 0.1% or better.

Both Voyager spacecraft will fly relatively close to Saturn (3.3 and $2.7R_S$) so that the Doppler frequency data taken at encounter, in combination with results from a successful close flyby of Saturn by Pioneer 11 in September, 1979, will yield information on the gravitational field of Saturn of comparable quality to that obtained for Jupiter in the Pioneer 10/11 missions. The second, third, and fourth zonal harmonic coefficients (J_2, J_3, J_4) will be determined to an accuracy of one part in 10^5 or better. A close encounter with Uranus could provide similar accuracies for the gravitational harmonics of that planet. The Jupiter results have been used to test the assumption that the planet is in hydrostatic equilibrium, and to limit the class of plausible interior models (Anderson *et al.*, 1974; Podolak and Cameron, 1974; Stevenson and Salpeter, 1976; Zharkov and Trubitsyn, 1976; Hubbard and Slattery, 1976). One of the most interesting features of the current Jupiter interior models is that they require several tens of Earth masses of elements heavier than helium to fit the gravitational data, at least if the solar ratio of the abundance of helium to hydrogen is retained. In any case, it is clear that Jupiter is not of solar compositon. We should similarly be able to determine the degree to which Saturn and Uranus deviate from solar composition. A comparison of the chemical compositions of these three giant planets will yield new clues to the formation process for all of the planets.

Preliminary mathematical model studies for the Saturn encounters indicate that the rings will not cause confusion in the determination of the gravitational harmonics for the planet. The results show that the determination of the total mass in the rings, as well as the separate mass in the A and B rings, is not significantly correlated with the planetary harmonics. It should be possible to determine the total mass in all of the rings to an accuracy of $\pm 8 \times 10^{-7}$ Saturn masses or better. The masses of the A and B rings should be resolvable individually to an accuracy of at least $\pm 2.4 \times 10^{-7}$ Saturn masses.

For the satellites of the outer planets, the accuracy in the determination of their masses depends on the distance of closest approach and on the relative spacecraft-satellite velocity. Plots of the percentage mass error are shown in Figure 5 for a flyby velocity of 20 km sec^{-1}. We have made the reasonable assumption that optical tracking has been used to improve the ephemerides of the satellites to a level where they are no longer an important error source in the mass determinations. In the figure, masses of a number of the satellites of Jupiter and Saturn are located along the horizontal axis. These values are taken from Newburn and Gulkis (1973). A line representing a sphere of lunar density is also shown on the plot to represent minimum possible flyby distances. In addition to improving the precision in the masses of the Galilean satellites, it will be possible with Voyager to determine the masses of some of the satellites of Saturn to an accuracy of better than 5%. Encounter conditions for the satellites of Uranus have not yet been planned.

The mean densities of the satellites are of fundamental interest. Thus both the mass and radius of the satellites must be found. From a consideration of radio and optical tracking determinations of the masses, and optical measurements of satellite radii, it appears that the determination of mean densities for Titan and the Galilean satellites will be limited by the size measurements, while for those smaller satellites of Jupiter and Saturn which have good optical coverage, mass uncertainties will be limiting. For the latter, Figure 5 can be used directly to estimate errors in mean densities. For a flyby velocity slower than the high estimate of 20 km s^{-1} used in Figure 5, the curves are shifted to the left and greater accuracy can be achieved.

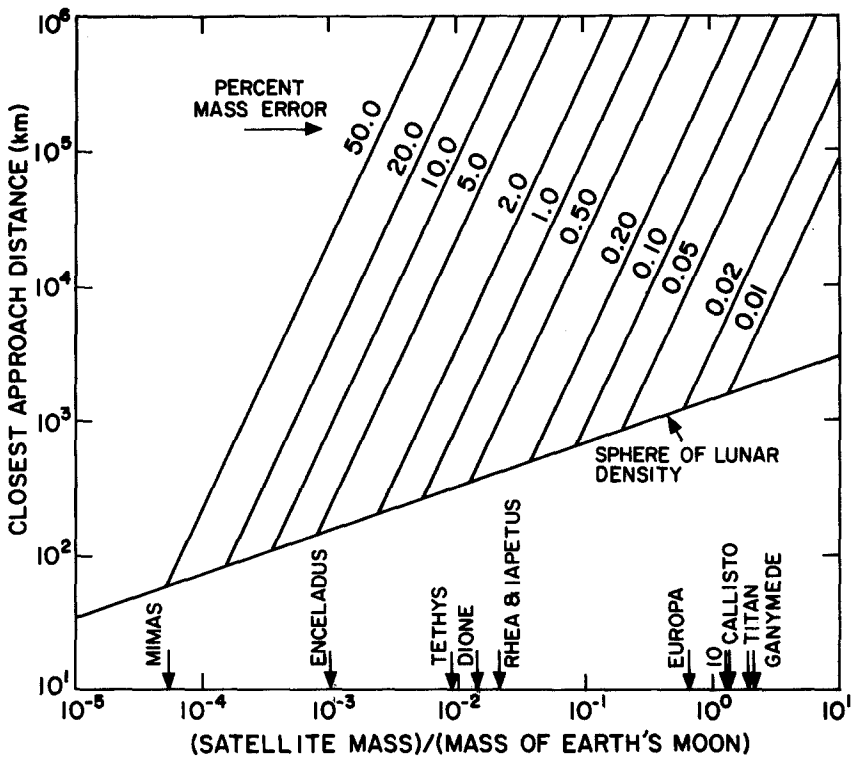

Fig. 5. Precision of mass determinations of various satellites. Percent error in computed mass is the parameter on the parallel lines, which are plotted on coordinates representing satellite mass and closest approach distance for an assumed spacecraft velocity of 20 km sec^{-1}. The masses of a number of satellites of Jupiter and Saturn are indicated: for example, the JSX flyby of Ganymede at 55 000 km should yield the mass to an accuracy of about 0.04%. Minimum possible flyby distances are represented by the 'sphere of lunar density' line.

Accurate densities for the satellites are very important for constructing models of these objects. High density bodies ($\rho > 3$) are probably rocky, silicate structures; low densities ($\rho < 2$) suggest a large percentage of ices. Lewis (1971a, b) has proposed

models of the Galilean satellites which make these bodies very unlike our own Moon. The Pioneer results suggesting a density of 3.5 for Io (Anderson *et al.*, 1974) may indicate that this object at least is of the more familiar type found in the inner Solar System. The density gradient in the satellites (decreasing outward from Jupiter) bears a qualitative similarity to that seen in the terrestrial planets relative to the Sun, and may have important cosmogonic implications.

5. Solar Corona and Interplanetary Medium

As the 13 and 3.5 cm-λ signals from the spacecraft pass through the solar corona on their journey to Earth, their group velocities decrease slightly below the speed of light because of the interaction with the free electrons in the corona. This effect is more pronounced at the longer wavelength than it is at the shorter. The difference of arrival time at Earth of the two signals sent simultaneoulsy from the spacecraft will be measured. From this difference and the known distance from Earth to the spacecraft, it is a straightforward matter to calculate the average number density of electrons along the path (Croft 1971). Furthermore, since the solar wind plasma consists predominantly of hydrogen and a small percentage of helium, the electron count can be converted with good accuracy into an equivalent density of plasma. By this method, we plan to use observations of differential group delay between the two signals as a means for monitoring the solar wind and coronal density between Earth and each Voyager spacecraft.

Except for the first months after launch, the two spacecraft will be close together in the sky as seen from Earth. Thus the two propagation paths lie close together and near the ecliptic plane during the long cruise to the outer Solar System. Since this will last 4 years or more, there will be numerous opportunities to carry out these observations when the spacecraft are near superior conjunction and the propagation paths lie near the Sun. The observations from this pair of spacecraft should provide excellent diagnostic data for determining the coronal shape and density and the large-scale flow patterns of the solar wind, particularly when the data are studied together with corollary observations from these and other spacecraft and from Earth observations which bear on this same set of phenomena.

One limitation of the 'dual-frequency experiment' (as this method of measurement has come to be called) is its sensitivity to solar wind density but not to speed. However, with two paths under surveillance and with our knowledge that the flow direction is always within a few degrees of the outward radial from the Sun (Hundhausen, 1972), it should be possible to complement the density with velocities derived from the observed delay between the onset of recognizable changes on the two paths.

Because the solar wind density decreases as it moves away from the Sun, roughly in inverse proportion to the square of the distance from the Sun, this type of path-average observation is most sensitive to conditions along those parts of the ray path

nearest the Sun. By virtue of the changing solar elongation of the Voyager spacecraft, it will be possible to carry out these observations at a variety of heliocentric distances many times during the progress of the missions.

As the signals from the spacecraft travel to Earth, they must traverse regions of turbulence and other forms of inhomogeneity in the solar wind and corona. As a result, the amplitude of the radio wave becomes nonuniformly distributed over its advancing front, and the front itself is rippled. The pattern of plasma inhomogeneity is convected outward due to the radial travel of the solar wind at a velocity of some 400 ± 200 km per second. A receiver immersed in the radio wave field thus senses a signal having unpredictably varying amplitude and phase. The overall effect is called Interplanetary Scintillation, IPS. The study of this phenomenon has proven fruitful as a means for determining the statistical characteristics of the solar wind turbulence and for the tracking of macroscopic flow patterns by virtue of the recognizably different degrees of turbulence in the travelling regions of plasma. Much of the study of IPS has been carried out through the observation of natural radio sources with the object of learning characteristics of the sources themselves through their influence on the IPS statistics.

The two signals from each Voyager spacecraft at the two wavelengths will provide diagnostic data of use in studying the character of interplanetary turbulence. Such two-frequency scintillation of spacecraft signals has been measured with Pioneer 9 (Chang, 1976), Mariner 10 (Howard *et al.*, 1975), and Viking (Tyler *et al.*, 1977), and it will also be done with Pioneer Venus (Colin and Hunten, 1977) in the same time frame as Voyager. However the Voyager pair of spacecraft offers the first access to dual-frequency radio signals from two neighboring points in the distant Solar System. In addition, the stability of the Voyager oscillators will make possible improved phase scintilation measurements. For the largest scale turbulence, it may be possible to observe pattern repetitions from one spacecraft signal to the other; from such correlation we can infer the outward traveling velocity of the turbulent regions. Aside from the diagnostic information that the four Voyager IPS data sources will provide, we have two other corollary sources of information: (1) From the differential delay measurement, we will determine the average electron density along the path. These are the same electrons which cause the scintillation by virtue of their inhomogeneity. Thus we will have a measurement not only of the average density but also of the variation of density along the path. (2) In the months before and after September 1979, four spacecraft will be in the same region of the sky roughly behind the Sun; both the Voyager spacecraft, Pioneer Venus, and Pioneer 11 (which will then be near Saturn). Plans are already being formulated for obtaining and correlating the Voyager and Pioneer Venus scintillation observations, and we hope to be able to obtain further correlative data from similar Pioneer 11 measurements during this same interval. Such multiple sources will offer the unparalled opportunity to observe scintillation of three point sources of dual-frequency signals plus the fourth single-frequency source, Pioneer 11. On two of these paths, the Voyager pair, electron content will also be measured.

6. Experimental Relativity

In the 15-year or so history of efforts to improve radiometric capabilities for radio science investigations with spacecraft, there has been a continuing interest in potential experimental tests of several phenomena predicted by the theory of relativity. These effects can manifest themselves by departures in measured Earth-spacecraft distances from Newtonian expectations that range from tens of kilometers, through meters and centimeters, on to apparently open-ended possibilities at sub-centimeter scales. The Voyager dual-frequency radio systems will be used to make more refined tests of large effects and to attempt detection of small ones.

There is a general relativistic time delay in the round-trip signals to a spacecraft at conjunction due to the gravitational field of the Sun. The detailed nature of this relativistic effect was first published by Shapiro (1964) who subsequently tested it with colleagues to an accuracy of $\pm 5\%$ using radar ranging to Mercury and Venus (Shapiro *et al.*, 1971). An improvement to $\pm 3\%$ was accomplished using radio ranging to Mariner 6/7 (Anderson *et al.*, 1975). For ray paths that pass near the Sun, the extra round trip delay is given by

$$\Delta t = \frac{2R_G}{c} \ln\left(\frac{4r_e r_p}{r_i^2}\right)$$

where r_e is the Sun–Earth distance, r_p is the Sun–spacecraft distance, and r_i is the impact parameter, the closest approach distance of the ray to the center of the Sun (Will, 1974). The gravitational radius $R_G = 2GM/c^2$ where M is mass and G is the gravitational constant. For the sun, $R_G = 2955$ m. To lowest order, the time delay (and the ray bending predicted in 1911 by Einstein) can be viewed classically as being due to a spherical relativistic 'atmosphere' surrounding the gravitating body, having a refractivity $\nu = R_G/r$ at radius r.

The time delay is maximum for ray paths that graze the Sun, for which condition it will vary from about 270 μsec for spacecraft at the distance of Jupiter, to about 300 μsec at the distance of Uranus. These time delays correspond to apparent increases in range of 40 and 45 km. While the predicted relativistic effect of the Sun has been tested to an accuracy of a few percent, there are two features of the Voyager missions which make additional measurements important. First of all, the dual frequency radio system will allow the removal of time delay effects caused by the solar plasma. Only the Viking orbiters have a similar capability, and it is expected that they will yield one measurement of the relativistic delay to better than $\pm 1\%$. The second advantage of Voyager is that the relativistic delay can be measured annually for the duration of the mission to an accuracy of better than 1%. If the Einstein theory is going to break down at the sub 1% level, then repeated measurements at varying geometries will be important for verification.

Another experiment is the general relativistic redshift of the spacecraft on-board oscillators caused by the gravity fields of Jupiter and Saturn. This effect can be measured to about $\pm 1\%$. While this is not competitive with similar experiments

referenced to atomic frequency standards on Earth-orbiting spacecraft (Vessot, 1974), the measurements at Jupiter and Saturn constitute independent and simpler tests. According to laboratory tests, the particle radiation environment at Jupiter will also cause a shift in the frequency of the spacecraft oscillator, and this may make the redshift measurement less reliable at Jupiter than at Saturn.

There is no doubt that the above effects can be measured to an accuracy which is a very small fraction of their total values. In the remainder of this section we discuss several effects which may be too small to be detected at all with Voyager. They are being considered nevertheless because the ultimate capabilities of the radio systems and of our analyses are not precisely known, and because of the intrinsic importance of the subject. The three effects discussed below involve a possible breakdown of the equivalence principle, the rotation of inertial coordinates near a massive spinning body, and gravitational waves.

A test of the equivalence principle may be possible from a measurement of the orbital parameters of Jupiter and the motions of the spacecraft and the Galilean satellites. It is known that the ratio of gravitational to inertial mass for a wide variety of small objects is unity to an accuracy of roughly one part in 10^{11}. The potential difference from one kind of object to another relates to differences in chemical composition, and hence essentially to differences in nuclear binding energy. In an analogous way, it is of interest to test for a possible change in this ratio due to a difference in gravitational binding energy, as suggested by Nordtvedt (1968a, b). This is best looked for with objects of large gravitational self-energy.

For the Earth, it has been found that the gravitational self energy contributes equally, $\pm 3\%$, to the inertial and passive gravitational masses, by using laser ranging to the Moon (Williams *et al.*, 1976; Shapiro *et al.*, 1976). For Jupiter, the ratio of gravitational binding energy to rest energy is about 35 times that for the Earth. The most direct effect of a breakdown in the equivalence principle for Jupiter would be that it would have a slightly different period-radius relationship as compared with the smaller inner planets and Kepler's third law. For example, for a given known period, there would be a discrepancy in the radius of Jupiter's orbit of about 4.3 km if the mass equivalence of the binding energy were contributing to either the inertial or the gravitational mass but not the other. It is not yet known whether this difference, and more subtle but related effects on spacecraft and satellite motions, can be determined to useful accuracies with Voyager.

Another general relativistic effect involves the mass current of a spinning central body, and the associated slow rotation of inertial coordinates with respect to distant 'fixed' stars, in inverse proportion to the cube of distance from the center of mass (Thirring, 1918). Radio waves travelling with the current on one side of the Sun would show a path length difference of up to several centimeters compared to a path against the current on the other side (Eshleman, 1973). The motion of spacecraft near Jupiter would also be affected, corresponding to a rotation of intertial coordinates of 150 m/year at $5R_J$, for example. No tests of these predicted effects have yet been made. Unfortunately, they are expected to be beyond the Voyager capabilities.

While there have been several very preliminary attempts to detect gravitational waves by their effects on radio link measurements, theoretical predictions of the likelihood and characteristics of such effects have been developed only relatively recently. A plane gravitational wave pulse crossing the solar system can produce a characteristic 3-pulse response in the two-way Doppler tracking signal of an interplanetary spacecraft. The shape of the response depends on the shape of the gravity wave pulse, on the Earth-spacecraft distance, and on the angle between the Earth-spacecraft direction and the propagation direction of the gravity wave (Estebrook and Wahlquist, 1975, 1976). The predicted signals must be detected in the presence of much larger Doppler noise resulting from plasma scintillations, spacecraft buffeting, clock errors, and the present level of accuracy of frequency generation and measurement. The major problem will be the elimination of noise due to the interplanetary plasma. The predicted unique signature of gravity pulses might permit data reduction techniques which can identify these signals in the presence of relatively large amounts of noise. The detection sensitivity for gravitational waves obtainable with the Doppler method is directly related to the precision with which the fractional frequency shift $\Delta f/f$ can be measured. The present system can achieve a basic accuracy of about 10^{-13} for this ratio on pulses having about one minute periods. Recent analyses by Thorne and Braginsky (1976), and a survey by Thorne (1977), have explored the possible sources of gravitational radiation with comparable periods. It does not appear likely from their calculations that gravitational waves will be detected with Voyager, but there is a large degree of uncertainty in the predictions. At least the present astrophysical theory allows the possibility of detectable pulses due to extremely energetic events, such as the collision of supermassive black holes.

7. Radio Science Instrumentation

The Voyager spacecraft incorporate several improvements to equipment and design that will enhance the radio science investigations with respect to previous planetary missions. These changes were motivated by the recognized difficulty in performing radio propagation observations at the outer planets, the complexity of the Voyager investigations, and a desire to advance the precision of radio science experiments for this and subsequent planetary and interplanetary spacecraft missions.

With these improvements, Voyager will have: coherent, high power, 3.5 and 13 cm wavelength amplifiers; increased spacecraft antenna size; a highly-stable, radiation-hardened, quartz frequency oscillator; improved phase and group delay stabilities in the spacecraft transponder; and a novel attitude control thruster configuration that minimizes spacecraft accelerations along the Earth-spacecraft line-of-sight. In addition, there are several other innovations affecting the practical, operational aspects of these investigations. Expected flight characteristics of the Voyager spacecraft radio systems are summarized in Table I.

TABLE I

Selected performance parameters for the Voyager spacecraft radio systems

Transmitting Parameters:	
Transmitting Frequencies (Nominal)	2295 MHz (S-band)
	8415 MHz (X-band)
Carrier Transponder	240/221 (S-band)
Turnaround Ratio	880/221 (X-band)
S/X Carrier Coherency Ratio	11/3
Transmitter Powers	9 Watts (S-band Low Power)
	26 Watts (S-band High Power)
	12 Watts (X-band Low Power)
	22 Watts (X-band High Power)
Transmitting Antenna Gain	36 dB (S-band)
(3.66 Meter Parabola)	47 dB (X-band)
Transmitting Polarization	Right Hand Circular (S-band)
	Right or Left Hand circular (X-band)
Transmitter Frequency Fluctuations	1 to 4×10^{-12} short term (see text)
(Ultra Stable Oscillator)	
Receiving Parameters:	
Receiving Frequency (Nominal)	2115 MHz
Receiving Antenna Gain	35 dB
(3.66 Meter Parabola)	
Receiving System Noise Temperature	2000 Kelvins
Receiving Polarization	Right Hand Circular
Carrier Tracking Loop	18 Hz
Threshold Noise Bandwidth	
Ranging Channel Noise Bandwidth	1.5 MHz

In general, these improvements have arisen to meet the needs of both spacecraft engineering and radio science. For example, increased radio signal strengths are needed for other engineering and science instruments, principally the telemetry requirements of the imaging system, and the new thruster configuration improves spacecraft navigation while aiding the celestial mechanics investigations.

The stabilized frequency reference represents the most dramatic improvement in radiometric performance. This unit (called the Ultra Stable Oscillator) is designed to achieve maximum frequency stability over time intervals of about 1 to 600 sec, the critical period for occultation events. The stability is specified in terms of the frequency deviation from a straight line fit to the oscillator drift over a 10 min period. The residuals to such fits, expressed in terms of fractional frequency changes, vary between about 1×10^{-12} and 4×10^{-12} with integration times between 1 and 10 sec. Oscillator long-term drift rates are about 5×10^{-11} per day under laboratory conditions, with uncertainties of about 1×10^{-11} per day.

Past occultation experiments with spacecraft radio communications systems have been conducted in two ways. Either the spacecraft transponder oscillator has been phase-locked to a reference signal transmitted from the ground, known as two-way mode, or, in the absence of such a reference signal, the transponders have automatically switched to a conventional auxiliary, quartz reference source. These two

reference schemes have achieved intermediate-term frequency stabilities of about 1×10^{-11} and 1 to 5×10^{-10} respectively. For deep atmospheres and in the vicinity of ionospheric caustics, two-way occultations suffer from the degraded performance of the spacecraft transponder under transient up-link signal conditions. Eventually the two-way locked condition is lost, and the resulting discontinuities in the switch to the on-board auxiliary reference, under thermally varying conditions, further impair the utility of the data. For Voyager, the stabilized frequency reference will surpass the past two-way conditions in terms of intermediate frequency stability, while providing several orders of magnitude reduction in sensitivity to changes in thermal and electrical environment and to radiation effects. Voyager occultations will be conducted using the new on-board oscillator as the frequency reference for the entire experiment, thus eliminating the above problems.

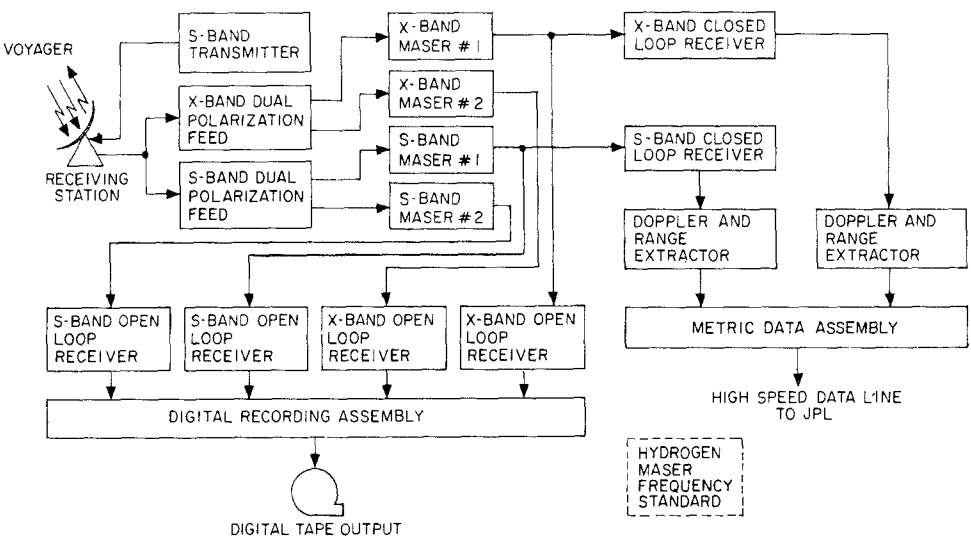

Fig. 6. Ground station functional block diagram for radio science during the Voyager missions.

The Deep Space Network (DSN), operated by JPL, provides the radio tracking stations for Earth-based measurements relating to the radio science investigations. The DSN consists of a world-wide network of stations having 26 m and 64 m diameter antennas. In support of the Voyager communications, navigation, and radio science requirements, the capabilities of the tracking stations are being improved to enhance the quantity and quality of received data. These improvements include the ability to simultaneously receive right- and left-hand circularly polarized 13 and 3.5 cm-λ signals with the 64 m antennas, real-time digitization of open-loop receiver outputs, programmed oscillator control of open loop receivers, non-real-time bandwidth reduction of open-loop recorded signals, and hydrogen maser frequency standards. An extensive research effort during the past year has improved

the accuracy of range measurements through development of improved calibration techniques and stabilized hardware configurations. The 26 m subnet of the DSN which is committed to Voyager support will be modified to receive X-band as well as S-band, and the antennas will be enlarged to 34 m in diameter.

In addition to the improved facilities, the tracking stations will also provide extensive measurements of engineering parameters associated with the acquisition of radio science data. These measurements will be displayed in real-time at the JPL mission control center at Pasadena, CA, and will allow interaction between the experimenters and the tracking stations. This will yield the visibility needed to adaptively conduct the radio science investigations. Expected performance for the DSN systems supporting radio science is summarized in Table II. A block diagram of selected elements at a 64 m tracking site is shown in Figure 6.

TABLE II
Selected performance parameters of a 64 m tracking station

Transmitting Parameters:	
Transmitting Frequency (Nominal)	2115 MHz
Transmitter Power	20 or 100 KW
Transmitter Antenna Gain (64 Meter Parabola)	60 dB
Transmitting Polarization	Right Hand Circular
Transmitter Frequency Stability (Hydrogen Maser)	2×10^{-14} for 12 hours
Maximum Range Code Frequency	Uplink Transmitter Frequency Divided by 4096
Receiving Parameters:	
Receiving Frequencies (Nominal)	2295 MHz (S-band) 8415 MHz (X-band)
Receiving Antenna Gain (64 Meter Parabola)	61 dB (S-band) 71 dB (X-band)
Receiving Noise Temperatures (Typical at Zenith)	22 Kelvins (S-band) 25 Kelvins (X-band)
Receiving Polarization	Right and/or Left Hand Circular (S-band) Right and/or Left Hand Circular (X-band)

Acknowledgements

The authors gratefully acknowledge the assistance and support of the Voyager project staff at the Jet Propulsion Laboratory of the California Institute of Technology and at NASA headquarters, the Deep Space Network personnel, and colleagues at their respective institutions. This work is being supported by NASA.

References

Anderson, J. D.: 1976, 'The Gravity Field of Jupiter' in T. Gehrels (ed.), *Jupiter*, U. Ariz. Press, Tucson, p. 113.

Anderson, J. D., Esposito, P. B., Martin, W., Thornton, C. L., and Muhleman, D. O.: 1975, *Astrophys. J.* **200**, 221.

Anderson, J. D., Hubbard, W. B., and Slattery, W. L.: 1974, *Astrophys. J.* **193**, L149.

Anderson, J. D., Null, G. W., and Wong, S. K.: 1974, *J. Geophys. Res.* **79**, 3661.

Chang, H.: 1976, Dissertation, Stanford University, Stanford, California.

Colin, L. and Hunten, D. M. (eds): 1977, *Space Sci. Rev.* **20**, 451.

Croft, T. A.: 1976, *Radio Sci.* **11**, 629.

Croft, T. A.: 1971, *Radio Sci.* **6**, 55.

Eshleman, V. R.: 1975, *Science* **189**, 876.

Eshleman, V. R.: 1974, 'The Mariner Jupiter/Saturn Ring Occultation Experiment' in F. D. Palluconi and G. H. Pettengill (eds.) *The Rings of Saturn*, NASA Sp-343.

Eshleman, V. R.: 1973, *Planet. Space Sci.* **71**, 1521.

Eshleman, V. R.: 1965, 'Radar Astronomy of Solar System Plasmas' in J. Aarons (ed.), *Solar System Radio Astronomy*, Plenum Press, New York, 267.

Eshleman, V. R. and Haugstad, B. S.: 1977, *Astrophys. J.* **214**, 928.

Estabrook, F. B. and Wahlquist, H. D.: 1976, paper A75-47 presented at 27th IAF Congress.

Estabrook, F. B. and Wahlquist, H. D.: 1975, *General Relativity and Gravitation* **6**, 439.

Fjeldbo, G. and Eshleman, V. R.: 1968, *Planet. Space Sci.* **16**, 1035.

Fjeldbo, G. and Eshleman, V. R.: 1965, *J. Geophys. Res.* **70**, 3217.

Fjeldbo, G., Eshleman, V. R., Gariott, O. K., and Smith, F. L. III: 1965, *J. Geophys. Res.* **70**, 3701.

Fjeldbo, G., Kliore, A. J., and Eshleman, V. R.: 1971, *Astron. J.* **76**, 123.

Fjeldbo, G., Kliore, A., Seidel, B., Sweetnam, D., and Woiceshyn, P.: 1976, 'The Pioneer 11 Radio Occultation Measurements of the Jovian Ionosphere', in T. Gehrels (ed.) *Jupiter*, U. Ariz. Press, Tucson, 238.

Goldstein, R. M., Green, R. R., Pettengill, G. H., and Campbell, D. B.: 1977, *Icarus* **30**, 104.

Haugstad, B. S.: 1977, 'Turbulence in Planetary Occultations: I. A Theoretical Formulation', submitted to *Icarus*.

Howard, H. T., Tyler, G. L., and Croft, T. A.: 1975, 'Corona Electron Concentration and Radio Scintillations Measured with the Mariner 10 Radio System', presented at 18th COSPAR, Varna, Bulgaria.

Howard, H. T., Tyler, G. L., Fjeldbo, G., Kliore, A. J., Levy, G. S., Brunn, D. I., Dickinson, R., Edelson, B. E., Martin, W. L., Stelzried, C. T., Sweetnam, D. N., Zygielbaum, A. I., Esposito, P. B., Anderson, J. D., Shapiro, I. I., and Reasenberg, R. D.: 1974, *Science* **183**, 1297.

Hubbard, W. B., Hunten, D. M., and Kliore, A. J.: 1975, *Geophys. Res. Letters* **2**, 265.

Hubbard, W. B. and Jokipii, J. R.: 1975, *Astrophys. J.* **199**, L193.

Hubbard, W. B. and Slattery, W. L.: 1976, 'Interior Structure of Jupiter: Theory of Gravity Sounding', in T. Gehrels (ed.), *Jupiter*, U. Ariz. Press, Tucson, 176.

Hundhausen, A. J.: 1972, in *Coronal Expansion and Solar Wind*, Springer Verlag, New York, 27.

Hunten, D. M. (ed.): 1974, *The Atmosphere of Titan*, NASA Sp-340.

Kliore, A. J., Cain, D. L., Levy, G. S., Eshleman, V. R., Drake, F. D., and Fjeldbo, G.: 1965, *Astronautics and Aeronautics*, July, 72.

Kliore, A. J. and Woiceshyn, P. M.: 1976, 'Structure of the Atmosphere of Jupiter from Pioneer 10 and 11 Occultation Measurements' in T. Gehrels (ed.), *Jupiter*, U. Ariz. Press, Tucson, 216.

Lewis, J. S.: 1971a, *Science* **172**, 1127.

Lewis, J. S.: 1971b, *Icarus* **15**, 174.

Marouf, E. A.: 1975, Dissertation, Stanford Univ. Stanford, California.

Newburn, R. L. and Gulkis, S.: 1973, *Space Sci. Rev.* **14**, 179.

Nordtvedt, K. Jr.: 1968a, *Phys. Rev.* **169**, 1014.

Nordtvedt, K. Jr.: 1968b, *Phys. Rev.* **170**, 1186.

Podolak, M. and Cameron, A. G. W.: 1974, *Icarus* **22**, 123.

Pollack, J. B.: 1973, *Icarus* **20**, 263.

Shapiro, I. I.: 1964, *Phys. Rev. Lett.* **13**, 789.
Shapiro, I. I., Ash, M. E., Ingalls, R. P., Smith, W. B., Campbell, D. B., Dyce, R. B., Jurgens, R. F., and Pettengill, G. H.: 1971, *Phys. Rev. Lett.* **26**, 1132.
Shapiro, I. I., Counselman, C. C. III, and King, R. W.: 1976, *Phys. Rev. Lett.* **36**, 555.
Stevenson, D. J. and Salpeter, E. E.: 1976, 'Interior Models of Jupiter' in T. Gehrels (ed.), *Jupiter*, U. Ariz. Press, Tucson, 238.
Thirring, H.: 1918, *Z. Phys.* **19**, 33.
Thorne, K. S.: 1977, *Astrophys. J.*, in press.
Thorne, K. S. and Braginsky, V. B.: 1976, *Astrophys. J.* **204**, L1.
Tyler, G. L., Brenkle, J. P., Komarek, T. A., and Zygielbaum, A. I.: 1977, *J. Geophys. Res.*, in press.
Vessot, R. F. C.: 1974, 'Lectures on Frequency Stability and Clocks and on the Gravitational Red-Shift Experiment' in B. Bertotti (ed.), *Experimental Gravitation*, Academic Press, New York, p. 111.
Will, C. W.: 1974, 'The Theoretical Tools of Experimental Gravitation' in Bertotti (ed.), *Experimental Gravitation*, Academic Press, New York, 1.
Williams, J. G., Dicke, R. H., Bender, P. L., Alley, C. O., Carter, W. E., Currie, D. G., Eckhardt, D. H., Faller, J. D., Kaula, W. M., Mulholland, J. D., Plotkin, H. H., Poultney, S. K., Shelus, P. J., Silverberg, E. C., Sinclair, W. S., Slade, M. A., and Wilkinson, D. T.: 1976, *Phys. Rev. Lett.* **36**, 551.
Young, A. T.: 1976, *Icarus* **27**, 335.
Zharkov, V. N. and Trubitsyn, V. P.: 1976, 'Structure, Composition, and Gravitational Field of Jupiter' in T. Gehrels (ed.), *Jupiter*, U. Ariz. Press, Tucson, 133.